Time-dependent Heavy-Quark Potential at Finite Temperature from Gauge/Gravity Duality

Tomoya Hayata,[1,2,*] Kanabu Nawa,[2,†] and Tetsuo Hatsuda[2,3,‡]

[1]*Department of Physics, The University of Tokyo, Tokyo 113-0031, Japan*
[2]*Theoretical Research Division, Nishina Center, RIKEN, Wako 351-0198, Japan*
[3]*IPMU, The University of Tokyo, Kashiwa 277-8583, Japan*

(Dated: November 22, 2012)

The potential between a heavy quark and an anti-quark inside the quark-gluon plasma (QGP) is studied on the basis of the gauge/gravity duality. A real-time complex potential $V_{Q\bar{Q}}(t,r)$ is derived from the Wilson loop with the Euclidean AdS_5 black hole metric. To make the analytic continuation from the imaginary time to the real time, specific variational configurations of the string world sheet in the Euclidean metric are introduced. Rapid approach of $V_{Q\bar{Q}}(t,r)$ to its stationary value is found at the time scale $t \simeq (\pi T)^{-1}$ independent of the 't Hooft coupling λ. Also, the imaginary part of $V_{Q\bar{Q}}(\infty,r)$ is found to be significant above the length scale $r = 1.72(\pi T)^{-1}$ independent of λ. Implications of these results to the properties of heavy quarkonia in QGP are briefly discussed.

PACS numbers: 12.38.Mh,11.25.Tq,25.75.Nq,14.40.Pq,11.10.Wx

High temperature quark-gluon plasma (QGP), whose properties are important to understand the physics of early Universe at $10^{-4} \sim 10^{-5}$ sec after the big bang, is actively studied in heavy-ion collision experiments at the Relativistic Heavy Ion Collider (RHIC) and the Large Hadron Collider (LHC). The experimental data suggest that QGP with the temperature (T) of a few hundred MeV is not a weakly interacting gas of quarks and gluons but rather a strongly-coupled quark-gluon plasma (sQGP) [1]. One of the key quantities which characterizes sQGP is a small ratio of shear viscosity to entropy density $\eta/s = 1/4\pi$ [2] obtained by using the holographic duality between $\mathcal{N} = 4$ super Yang-Mills theory and the classical supergravity on $\mathrm{AdS}_5 \times \mathrm{S}^5$ [3]. Another physical quantity which can probe sQGP is the spectra of heavy quarkonia at finite T [4]. Such a probe was originally proposed in the context of the string breaking and Debye screening at finite T [5, 6]. Later, the lattice quantum chromodynamics (QCD) simulations [7] and the QCD sum rule analyses [8] on the basis of Bayesian technique have been attempted to study the melting pattern of quarkonia. It was also realized that the heavy-quark potential at finite T can be defined from the *Minkowski* Wilson loop in thermal medium: The potential thus defined is found to be *time-dependent* and *complex* by using thermal perturbation theory [9] and lattice QCD simulations [10]. (See also Ref. [11].)

The purpose of this Letter is to derive such a time-dependent complex potential at finite T in sQGP on the basis of the gauge/gravity duality in the large N_c and large 't Hooft coupling $\lambda = g^2_{\mathrm{YM}} N_\mathrm{c}$. We start with an *Euclidean* Wilson loop $W_\mathrm{E}(\tau, r)$ (τ (r) is the temporal (spatial) extent with $0 \le \tau < \beta = 1/T$) defined in the *Euclidean* AdS_5 black hole metric. After evaluating $W_\mathrm{E}(\tau, r)$ by its gravity dual following the Maldacena's conjecture [12], we carry out an analytic continuation to obtain the *Minkowski* Wilson loop $W_\mathrm{M}(t, r)$ with real-time t. Then, we can extract the characteristic time and length associated with the complex heavy-quark potential $V_{Q\bar{Q}}(t, r)$ obtained from $W_\mathrm{M}(t, r)$. We will discuss the role of the imaginary part of the potential for the quarkonium melting in our approach. We note that there is a previous attempt to derive a complex potential by using the gauge/gravity duality [13] under *Minkowski* AdS_5 black hole metric: We will mention its relation to our approach and also its limitation in studying the time-dependent phenomena.

Let us start with the rectangular Wilson loop $W_\mathrm{E}(\tau, r)$ in the Euclidean space-time and its spectral decomposition [10];

$$W_\mathrm{E}(\tau, r) = \lim_{M\to\infty} \int_{-2M}^{\infty} \mathrm{d}\omega\ \mathrm{e}^{-\omega\tau} \rho(\omega, r). \tag{1}$$

Here M is a bare heavy-quark mass taken to infinity at the end, and $\rho(\omega, r)$ is the spectral function of the heavy $Q\bar{Q}$ with relative distance r in thermal environment. The frequency ω denotes energy relative to $2M$, so that the spectral peaks of $\rho(\omega, r)$ associated with the bound and resonance states are located around $\omega = 0$ after appropriate subtraction of the heavy-quark self-energy in the spatial direction.

The time-dependent complex potential $V_{Q\bar{Q}}(t, r)$ at finite T in the Minkowski space-time is obtained from the analytic continuation of Eq.(1), $W_\mathrm{M}(t, r) = W_\mathrm{E}(\tau \to it, r)$, [9, 10];

$$V_{Q\bar{Q}}(t, r) = i\partial_t \ln W_\mathrm{M}(t, r) \tag{2}$$

$$= \frac{\int_{-\infty}^{\infty} \mathrm{d}\omega\ \mathrm{e}^{-i\omega t} \omega \rho(\omega, r)}{\int_{-\infty}^{\infty} \mathrm{d}\omega\ \mathrm{e}^{-i\omega t} \rho(\omega, r)}. \tag{3}$$

Although $\rho(\omega, r)$ and $W_\mathrm{E}(\tau, r)$ are both real and positive, $W_\mathrm{M}(t, r)$ and the real-time potential $V_{Q\bar{Q}}(t, r)$ become complex after the analytic continuation. The major questions to be addressed in this Letter are (i) how fast the real-time potential approaches to its asymptotic value as a function of t in sQGP? and (ii) what would be the typical time-scale and length scale characterizing the imaginary part of the potential?

To evaluate $W_\mathrm{E}(\tau, r)$, we follow the Maldacena's conjecture [12] and consider the gravity dual description of $W_\mathrm{E}(\tau, r)$ given by the extremum of the Nambu-Goto (NG) action in the background metric of the classical supergravity;

$$W_\mathrm{E}(\tau, r) = \mathrm{e}^{-S_\mathrm{NG}(\tau, r, X^\mu)}, \tag{4}$$

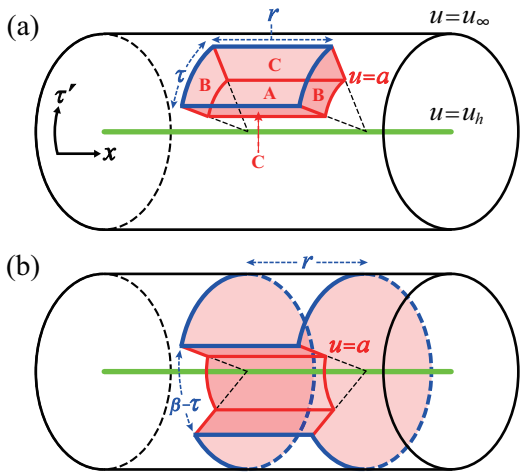

FIG. 1. (color online) Configuration ansatz of world sheet in the AdS_5 black hole metric with a rectangular contour on the boundary. Configurations I, II, and III corresponds to (a) with $a > u_h$, (a) or (b) with $a = u_h$, and (b) with $a > u_h$, respectively.

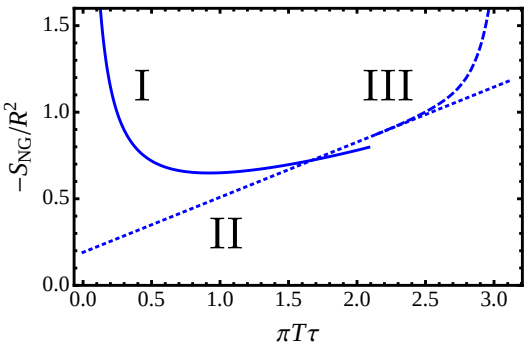

FIG. 2. (color online) Wilson loop as a function of the Euclidean time τ for $r = 1.0/\pi T$. The solid, the dotted and the dashed lines correspond to the configurations I, II and III, respectively.

where X^μ $(\mu = 0, \ldots, 4)$ are the coordinates of string world sheet embedded in the 5-dimensional Euclidean space-time with a finite rectangular contour on the boundary. These coordinates satisfy the equation of motion $\delta S_{\rm NG}/\delta X^\mu = 0$. We adopt the Euclidean AdS_5 black hole metric as a dual description for a strongly-coupled large $N_{\rm c}$ gauge theory at finite T;

$$ {\rm d}s^2 = \alpha' \Big[\frac{u^2}{R^2} \Big\{ f(u) {\rm d}\tau'^2 + {\rm d}\boldsymbol{x}^2 \Big\} + \frac{R^2}{u^2} \frac{{\rm d}u^2}{f(u)} \Big], \qquad (5) $$

where $\alpha' = \ell_s^2$ with ℓ_s being the string length and $f(u) = 1 - u_h^4/u^4$ with $u_h = \pi T R^2$ being the location of the event horizon in the fifth coordinate. $R = (2\lambda)^{1/4}$ is a radius in the string unit.

It is a formidable task to solve analytically the partial differential equation for string world sheet with finite rectangular contour on its boundary. Even if one could solve the problem numerically, it is not trivial to make an analytic continuation $\tau \to it$ only with the numerical data of $W_{\rm E}(\tau, r)$ even by using the Bayesian technique [10]. In this Letter, we take a variational approach to solve the string world sheet within specific configurations, so that one can pick up qualitative features of the Euclidean solution as well as its analytic continuation. The NG action in Eq. (4) is proportional to the area of the world sheet. Therefore, taking specific configurations corresponds to an approximate calculation of the area.

For small τ, we consider a variational configuration I (box type) shown in Fig. 1(a): It has only one variational parameter, the bottom stringy coordinate a in the fifth direction. As τ grows, another configuration II (wedge type) having $a = u_h$ would be relevant. For τ gets close to β, we consider the variational configuration III (anti-box type) shown in Fig. 1(b). In the limit $\tau \to \beta$, I (III) approaches to hanging configuration (two disconnected disks) of world sheet for the Polyakov loop correlator in Ref. [14].

By substituting the configurations I and III into the NG action, we obtain a closed form with a single variational parameter a. For example, the configuration I gives

$$ S_{\rm NG}^{\rm (I)}(\tau, r, a) = \frac{1}{2\pi} \Big[\tau r \frac{a^2}{R^2} \sqrt{f(a)} - 2\tau(a - u_\infty) $$
$$ + 2r \Big(\int_a^{u_\infty} {\rm d}u \, \frac{1}{\sqrt{f(u)}} \Big) - 2(\tau + r) u_\infty \Big] \qquad (6) $$
$$ = \frac{1}{2\pi} \Big[\tau r \frac{a^2}{R^2} \sqrt{f(a)} - 2\tau a - 2ra F(-\frac{1}{4}, \frac{1}{2}, \frac{3}{4}; \frac{1}{a^4}) \Big], \qquad (7) $$

with F being the Gauss hypergeometric function. First, second and third terms of Eq. (6) come from the area A, B and C in Fig. 1(a), respectively. The forth term in Eq. (6) corresponds to the subtraction of the quark self-energy $2u_\infty(\tau + r)/2\pi$ in the the temporal and spatial direction [12]: The action becomes finite for $u_\infty \to \infty$ after this subtraction. The extremum condition $\delta S_{\rm NG}^{\rm (I)}/\delta a = 0$ given τ and r reads

$$ \bar{a} - \frac{1}{\tau} = \frac{1}{r} \sqrt{1 - \Big(\frac{\pi T}{\bar{a}} \Big)^4 }. \qquad (8) $$

where a scaled coordinate $\bar{a} = a/R^2$ is introduced to eliminate λ. Similar equation can be derived for $a(\tau, r)$ of the configuration III [15].

In Fig. 2, we plot $W_{\rm E}(\tau, r)$ obtained by minimising $S_{\rm NG}$ in each configuration as a function of τ with fixed r. We consider only the real solution of $a(\tau, r)$ as physically acceptable one in the Euclidean space-time. It turns out that such a real solution of $a(\tau, r)$ disappear for configuration I (III) for large (small) τ [16]. Although the configurations I, II and III are not connected smoothly, either the extended variational configurations and/or the fluctuations of string world sheet would eventually remove the non-smoothness. If we consider the branch with larger value of $-S_{\rm NG}$ given τ in Fig. 2, the result is qualitatively consistent with that obtained from lattice QCD simulations [10]. Note that $\ln W_E(\tau, r)$ behaves as $\frac{1}{\tau}$ $(\frac{1}{\beta - \tau})$ at $\tau \to 0$ $(\tau \to \beta)$. However, it it is not symmetric with respect to $\tau = \beta/2$ in contrast to the case of the spatial Wilson line correlator.

Let us now consider the analytic continuation of $W_E(\tau, r)$. Within our variational approach, it is equivalent to the analytic

continuation of $a(\tau, r)$ by solving the master equation such as Eq. (8) with $\tau \to it$. Under the situation that the configurations I, II and III are continuous but not smooth, we primarily utilize the configuration I for describing the short time behavior of the potential. Furthermore, for large t and r, $V_{Q\bar{Q}}(t, r)$ obtained from I is found to have the same asymptotic behavior with that obtained from III. Namely, the configuration I has correct information both at small t and large t. Better variational configuration with a smooth interpolation among I, II and III is left for future studies.

Under the reservation mentioned above, we solved Eq.(8) numerically with $\tau \to it$ and found a *unique* solution $a(it, r)$ consistent with $a(\tau \sim 0, r) = \sqrt{2\lambda}/\tau + \cdots$ for the configuration I. Substituting the solution into Eq. (7), we can get the real-time Wilson loop $W_{\rm M}(t, r)$ as an analytically continued thermal Wilson loop, $W_{\rm E}(it, r)$. Then, by using Eq.(2), the real-time complex potential obtained from I reads

$$V_{Q\bar{Q}}(t, r) = -\frac{\sqrt{2\lambda}}{2\pi r}\left[2r\bar{a}(it, r) - (r\bar{a}(it, r))^3 + i\frac{r}{t}(r\bar{a}(it, r))^2\right]. \quad (9)$$

Since $\bar{a}(it, r)$ does not depend on λ, the potential is proportional to $\sqrt{\lambda}$ irrespective of the values of T, r and t. Note here that $a(it, r)$ is complex, while $a(\tau, t)$ is real: This is the reason why $V_{Q\bar{Q}}(t, r)$ can become complex despite the fact that the Euclidean Wilson loop $W_{\rm E}(\tau, r)$ is real.

To check if the above potential is consistent with the known result, we consider the asymptotic limit $t \to \infty$ at $T = 0$ in Eq. (9): In this case, $\bar{a}(it, r) \to 1/r$ as can be easily seen from Eq.(8), so that we obtain,

$$V_{Q\bar{Q}}(\infty, r)\Big|_{T=0} = -\frac{1}{2\pi}\frac{\sqrt{2\lambda}}{r}. \quad (10)$$

This is the same as that given in [12] except that the numerical coefficient $\frac{1}{2\pi}$ due to the box-type ansatz is smaller by 30% than the exact value $\frac{4\pi^2}{\Gamma(1/4)^4}$.

The time-dependence of the real and imaginary parts of the potential obtained from Eq. (9) are plotted in Fig. 3 for typical distances $r = 1/(\pi T), 2/(\pi T)$ and $3/(\pi T)$. Irrespective of the values of r, asymptotic values are found to be reached quickly near the equilibration time $t_{\rm eq}$ given by

$$t_{\rm eq} \simeq \frac{1}{\pi T}. \quad (11)$$

Note that $t_{\rm eq}$ is independent of λ, since $\bar{a}$ and $V_{Q\bar{Q}}(t, r)/\sqrt{2\lambda}$ are λ-independent. This is in contrast to the case of weakly-coupled QGP (wQGP) at $N_c = 3$ where we have $t_{\rm eq} \simeq 10/m_{\rm D} \sim 10/(gT)$ for $r = (1 \sim 3)/(\pi T)$ (see Fig.1 of the second reference in [9]). Here the Debye mass is defined by $m_{\rm D} = gT\sqrt{1 + N_f/6}$. One finds that $t_{\rm eq}$ in sQGP is not only parametrically different from that in wQGP, but also an order of magnitude shorter than that in wQGP.

The equilibration time $t_{\rm eq}$ can be regarded as a time-scale of the strongly coupled gluonic plasma to relax to its equilibrium state under the external disturbance caused by a color-singlet heavy $Q\bar{Q}$ with separation distance r at $t = 0$. Taking typical QGP temperature $T = 300$MeV at RHIC and LHC in Eq.(11), we have $t_{\rm eq} \simeq 0.22$ fm: This is comparable to the formation time of the low-lying heavy quarkonia from hard-process and also the phenomenological formation time of QGP obtained from relativistic hydrodynamics [1], so that the propagation of the heavy quarkonia in sQGP may well be described by using the complex potential in the asymptotic (static) limit.

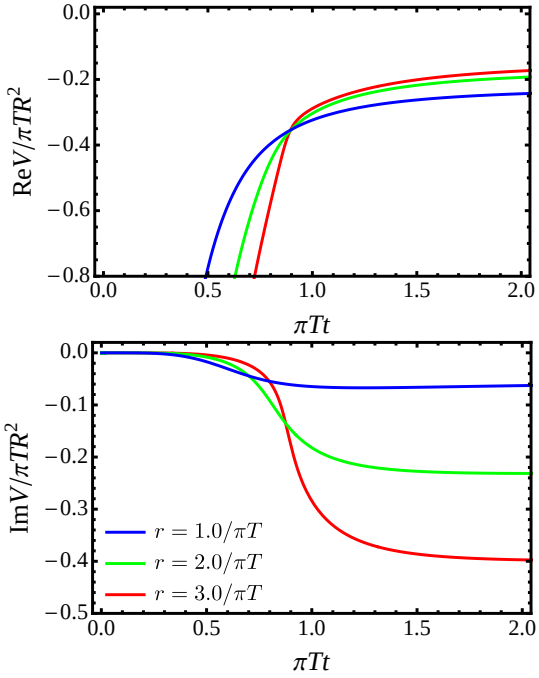

FIG. 3. (color online) Real and imaginary parts of the potential as a function of the real time t for $r = 1.0/\pi T$, $2.0/\pi T$ and $3.0/\pi T$.

It is in order here to comment on the relation between our approach with the Euclidean AdS_5 black hole metric and that with the Minkowski AdS_5 black hole metric. Our method is based on the spectral decomposition of the Euclidean Wilson loop and its analytic continuation to the real-time on the basis of a well-established formula in thermal field theory. On the other hand, if one starts from the Minkowski Wilson loop naively, one encounters a difficulty to select an appropriate solution [13]: Indeed, one needs to take into account real-time boundary conditions carefully [17]. One of the advantages of our Euclidean approach is that one can single out a unique configuration among various complex solutions appearing in the Minkowski approach. In fact, all what we need in our approach is to consider the *real* stationary configuration obtained from the extremum of the NG action with imaginary time τ, and then make an analytic continuation to the real-time t.

In Figure 4, we show the real and imaginary parts of the static potential after equilibration for different values of T. We normalise the potential by $\pi T_0 R^2$ and plot it as a function of $\pi T_0 r$, so that the curves are λ independent. Here T_0 is an arbitrarily energy scale.

At short distance, $\mathrm{Re}V_{Q\bar{Q}}(\infty, r)$ shows Coulomb-type behavior given by Eq.(10) irrespective of T. On the other hand, at long distance, the potential becomes deeper as T increases: This is consistent with what has been found in lattice QCD simulations where the large r behavior is dictated by twice of the thermal part of single-quark free energy $2F_Q(T)$ [18]. Note that such a deepening of the real part at long distances can be also seen in [13] if we use the same definition of $\mathrm{Re}V_{Q\bar{Q}}$ as ours by subtracting only the T-independent divergence due to the bare quark mass. We should remark here that the real part of our potential has a long tail $\sim r^{-1/3}$ at large r and does not approach to a constant. This may be related to the limitation of our simple box-type ansatz.

We find that the imaginary part of the potential shown in Fig. 4 , $\mathrm{Im}V_{Q\bar{Q}}(\infty, r)$, emerges at the threshold distance

$$r_{\mathrm{th}} = \left(\frac{4}{27}\right)^{1/4} \frac{1}{\pi T}. \tag{12}$$

Then, it grows linearly $\mathrm{Im}V_{Q\bar{Q}}(\infty, r \gg r_{\mathrm{th}}) \to -\frac{\sqrt{2\lambda}}{2\pi}(\pi T)^2 r$. This is qualitatively consistent with that obtained in [13]. Let us now define a "dissociation" distance r_{dis} where the imaginary part of the potential starts to dominate over the real part: For large t, Eq.(8) shows that $r\bar{a}$ is a function of $\pi T r$ only. Therefore, the condition $\mathrm{Re}V_{Q\bar{Q}}(\infty, r_{\mathrm{dis}}) = \mathrm{Im}V_{Q\bar{Q}}(\infty, r_{\mathrm{dis}})$ leads to a λ independent relation,

$$r_{\mathrm{dis}} = \frac{1.72}{\pi T}. \tag{13}$$

By taking typical QGP temperature $T = 300$ MeV at RHIC/LHC, we have $r_{\mathrm{dis}} \simeq 0.36$ fm. This is smaller than the Q-$\bar{Q}$ distance 0.5 fm for J/Ψ and 0.56 fm for Υ(2S) but is larger than 0.28 fm for Υ(1S) [19]. (For the estimate of the spatial sizes of heavy quarkonia, see Table 3 in [6].) This indicates that the sequential melting of heavy quarkonia seen in the relativistic heavy-ion collision experiments may be closely related to the physics of the imaginary $Q\bar{Q}$ potential rather than the color Debye screening. Detailed phenomenological studies are, however, necessary to make quantitative comparison between the theory and experiments [20].

In this Letter, we have presented a variational derivation of the time-dependent complex potential between heavy quarks $V_{Q\bar{Q}}(t, r)$ in the strongly-coupled QGP on the basis of the gauge/gravity duality. Our starting point is a rectangular Wilson loop in Euclidean space-time, $W_{\mathrm{E}}(\tau, r)$. Associated classical configurations of the string world sheet under the Euclidean AdS_5 black hole metric were evaluated variationally with a single parameter $a(\tau, r)$ in the fifth dimension. We derived a simple algebraic equation for $a(\tau, r)$ which allows us to carry out the analytic continuation of $W_{\mathrm{E}}(\tau, r)$ to obtain the real-time Wilson loop $W_{\mathrm{M}}(t, r)$: Its logarithmic derivative with respect to the real-time t is nothing but $V_{Q\bar{Q}}(t, r)$. Technically, the potential receives an imaginary part due to the process of analytic continuation.

Resultant $V_{Q\bar{Q}}(t, r)$ is found to have interesting properties. It shows a characteristic equilibration time $t_{\mathrm{eq}} \simeq (\pi T)^{-1}$ which is an order of magnitude smaller than the value obtained from the weak-coupling thermal perturbation theory. Also, the imaginary part of the potential starts to dominate over the real part at the distance $r_{\mathrm{dis}} = 1.72(\pi T)^{-1}$ which is comparable to the Q-$\bar{Q}$ distance of the low-lying heavy quarkonia. The above time scale and the length scale indicate the validity of using t-independent heavy quark potential in sQGP and the relevance of the imaginary part of the potential on the sequential melting of heavy quarkonia in sQGP, respectively.

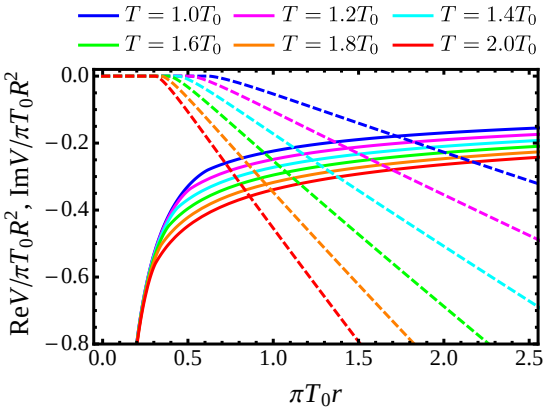

FIG. 4. (color online) The complex heavy-quark potential in the asymptotic limit ($t \to \infty$) as a function of the separation r. The solid and the dashed lines correspond to the real and the imaginary parts of the potential, respectively. T_0 is an arbitrary energy scale.

We have several future directions to improve our analyses presented in the Letter. First of all, we need to extend our variational configurations so that a single smooth function for $W_{\mathrm{E}}(\tau, r)$ is obtained. It would be also necessary to check the validity of various variational ansatz by solving the equation of motion in Euclidean metric numerically without approximation. Such a numerical solution may be also used to reconstruct the spectral function $\rho(\omega, r)$ by the Bayesian technique (e.g. the Maximum Entropy Method).

The authors thank H. Ooguri, Y. Imamura, S. Nakamura, M. Natsuume, A. Miwa, Y. Hidaka and Y. Kim for stimulating discussions and helpful comments. T. Hayata is supported by JSPS Research Fellowships for Young Scientists. K. Nawa is supported by the Special Postdoctoral Research Program of RIKEN. T. Hatsuda is supported in part by MEXT Grant-in-Aid for Scientific Research on Innovative Areas (No.2004:20105003) and by JSPS Grant-in-Aid for Scientific Research (B) No.22340052.

* hayata@riken.jp
† knawa@riken.jp
‡ thatsuda@riken.jp

[1] Reviewed in S. Sarkar, H. Satz and B. Sinha, Lect. Notes Phys. **785**, 1 (2010).

[2] P. Kovtun, D. T. Son and A. O. Starinets, Phys. Rev. Lett. **94**, 111601 (2005). Reviewed in J. Casalderrey-Solana *et al.*, arXiv:1101.0618[hep-th].

[3] J. M. Maldacena, Adv. Theor. Math. Phys. **2**, 231 (1998).

[4] For recent quarkonia results at RHIC and LHC, A. Adare *et al*. [PHENIX Collaboration], Phys. Rev. Lett. **98**, 232301 (2007); S. Chatrchyan *et al*. [CMS Collaboration], Phys. Rev. Lett. **107**, 052302 (2011); B. Abelev *et al*. [ALICE Collaboration], Phys. Rev. Lett. **109**, 072301 (2012).

[5] T. Hashimoto *et al.*, Phys. Rev. Lett. **57**, 2123 (1986); T. Matsui and H. Satz, Phys. Lett. B **178**, 416 (1986).

[6] Reviewed in H. Satz,J. Phys. G **32**, R25 (2006).

[7] M. Asakawa and T. Hatsuda, Phys. Rev. Lett. **92**, 012001 (2004); S. Datta *et al.*, Phys. Rev. D **69**, 094507 (2004); T. Umeda, K. Nomura and H. Matsufuru, Eur. Phys. J. C **39S1**, 9 (2005); G. Aarts *et al.*, JHEP **1111**, 103 (2011); H. T. Ding *et al.*, Phys. Rev. D **86**, 014509 (2012).

[8] P. Gubler, K. Morita and M. Oka, Phys. Rev. Lett. **107**, 092003 (2011); K. Suzuki, P. Gubler, K. Morita and M. Oka, arXiv:1204.1173 [hep-ph].

[9] M. Laine *et al.*, JHEP **0703**, 054 (2007); M. Laine, JHEP **0705**, 028 (2007); A. Beraudo, J. -P. Blaizot and C. Ratti, Nucl. Phys. A **806**, 312 (2008); N. Brambilla, J. Ghiglieri, A. Vairo and P. Petreczky, Phys. Rev. D **78**, 014017 (2008) [arXiv:0804.0993 [hep-ph]].

[10] A. Rothkopf, T. Hatsuda and S. Sasaki, PoS LAT **2009**, 162 (2009); Phys. Rev. Lett. **108**, 162001 (2012).

[11] C. Young and K. Dusling, arXiv:1001.0935 [nucl-th]; Y. Akamatsu and A. Rothkopf, Phys. Rev. D **85**, 105011 (2012); N. Borghini and C. Gombeaud, Eur. Phys. J. C **72**, 2000 (2012); N. Dutta and N. Borghini, arXiv:1206.2149 [nucl-th]; Y. Akamatsu, arXiv:1209.5068 [hep-ph].

[12] J. M. Maldacena, Phys. Rev. Lett. **80**, 4859 (1998).

[13] J. L. Albacete, Y. V. Kovchegov and A. Taliotis, Phys. Rev. D **78**, 115007 (2008); H. R. Grigoryan, Y. V. Kovchegov, Nucl. Phys. B **852**, 1 (2011). See also, J. Noronha and A. Dumitru, Phys. Rev. Lett. **103**, 152304 (2009).

[14] S. J. Rey, S. Theisen and J. T. Yee, Nucl. Phys. B **527**, 171 (1998); A. Brandhuber *et. al.*, Phys. Lett. B 434, 36 (1998).

[15] K. Nawa, T. Hayata and T. Hatsuda, in progress.

[16] For configuration I, there exist two real solutions, a local minimum and a local maximum of $S_{\rm NG}$. For large $\pi T\tau$, they undergo a pair annihilation and the real solution disappears. However, such an annihilation happens only after the configuration II takes over the configuration I. As for the configuration III, the real solution does not appear for $\pi T\tau < \pi - 1$. Furthermore, the configurations II and III take the same $S_{\rm NG}$ at $\pi T\tau = \pi - 1$.

[17] C. P. Herzog and D. T. Son, JHEP **0303**, 046 (2003).

[18] See e.g., Y. Maezawa *et al.*, arXiv:1112.2756 [hep-lat], to appear in Prog. Theor. Phys. (2012)

[19] If we identify $r_{\rm dis}$ with the typical Q-$\bar{Q}$ distances in the heavy quarkonia, we find $T_{\rm dis} = 390$, 220 and 190 MeV for Υ(1S), J/Ψ and Υ(2S), respectively.

[20] See e.g., P. Petreczky, C. Miao and A. Mocsy, Nucl. Phys. A **855**, 125 (2011); M. Strickland and D. Bazow, Nucl. Phys. A **879**, 25 (2012); F. Brezinski and G. Wolschin, Phys. Lett. B **707**, 534 (2012); A. Emerick, X. Zhao and R. Rapp, Eur. Phys. J. A **48**, 72 (2012).